SCIEPublish

Perspective

Perspectives on the Development in the Selective Oxidation of Glycerol to Value-Added Chemicals via Photoelectrocatalysis Coupled with Hydrogen Evolution

Xiaoyan Zhang *

Department of Chemistry, College of Sciences, Shanghai University, Shanghai 200444, China

* Corresponding author. E-mail: xyzhang_dd@shu.edu.cn (X.Z.); Tel.: +86-136-5165-4899 (X.Z.)

Received: 1 December 2024; Accepted: 10 March 2025; Available online: 1 April 2025

ABSTRACT: Harvesting sunlight to produce clean hydrogen fuel remains one of the main challenges for solving the energy crisis and ameliorating global warming. Photoelectrochemical (PEC) water splitting is considered to be a promising method for H_2 production in the future. However, the efficiency still remains challenging due to the sluggish reaction dynamics for water oxidation. Recently, the thermodynamically favorable oxidation of glycerol in PEC systems has gained significant attention for its ability to produce value-added chemicals while simultaneously generating hydrogen. This process not only enhances the yield of high-value products but also minimizes energy consumption and reduces CO_2 emissions. Valuable products from glycerol oxidation include 1,3-dihydroxyacetone (DHA), glyceraldehyde (GLD), tartronic acid (TA), formic acid (FA), and glyceric acid (GA). Thus, it is important to improve selectivity and productivity. In this work, we mainly summarize the recent research progress in improving the selectivity and productivity of glycerol upgrading products on the different photoanodes.

Keywords: Photoelectrocatalysis; PEC glycerol oxidation; Value-added chemicals; H_2 production

1. Introduction

Photoelectrochemical (PEC) cells provide promising approaches for saving natural solar energy in the conversion of H_2O, N_2, and CO_2 into H_2, NH_3, and low-carbon fuels, etc., at the cathode [1–3]. Nevertheless, the sluggish 4-electron transfer of the oxygen evolution reaction (OER) at the anode affects the reduction reactions and limits the overall efficiency. Therefore, instead of the OER, rapid oxidation reactions generating value-added products have been explored in recent years [4]. Glycerol, as a residual by-product of biodiesel, can be upgraded into high-value-added building blocks via mild catalytic reactions powered by renewable energy resources (Figure 1) [5]. Therefore, PEC glycerol oxidation (GOR) has drawn attention recently among various PEC organic upgrading reactions.

As one of the 12 high-value biobased platform chemicals designated by the U.S. Department of Energy, glycerol is pivotal in enhancing the "photon economy" due to its high reaction rate and yield of value-added products. The valuable products include 1,3-dihydroxyacetone (DHA), glyceraldehyde (GLD), tartronic acid (TA), formic acid (FA), glyceric acid (GA), and lactic acid (LA). The price of FA and DHA is about 1.0 and 148.75 USD per kg, respectively, about dozens of times and thousands of times that of oxygen, which is around 0.04 USD per kg [6]. It should be noted that the above comparison neglects the separation cost of GOR products. Moreover, GOR is more favorable in thermodynamics and kinetics. For example, the oxidation potential of glycerol to DHA is at 0.40 V *vs.* SHE, which is significantly lower compared to that of H_2O at 1.23 V *vs.* SHE [7]. Consequently, the GOR is considered to be a superior alternative to the traditional OER to PEC hydrogen evolution, offering high energy conversion efficiency and long-term stability of PEC cells [8]. To achieve superior PEC performance, the semiconductors used in photoelectrodes should possess a sufficiently wide band gap, high catalytic activity, and chemical stability. To date, many excellent reviews have been reported on PEC glycerol upgrading coupled with H_2 production [5,9–11].

https://doi.org/10.70322/prp.2025.10009

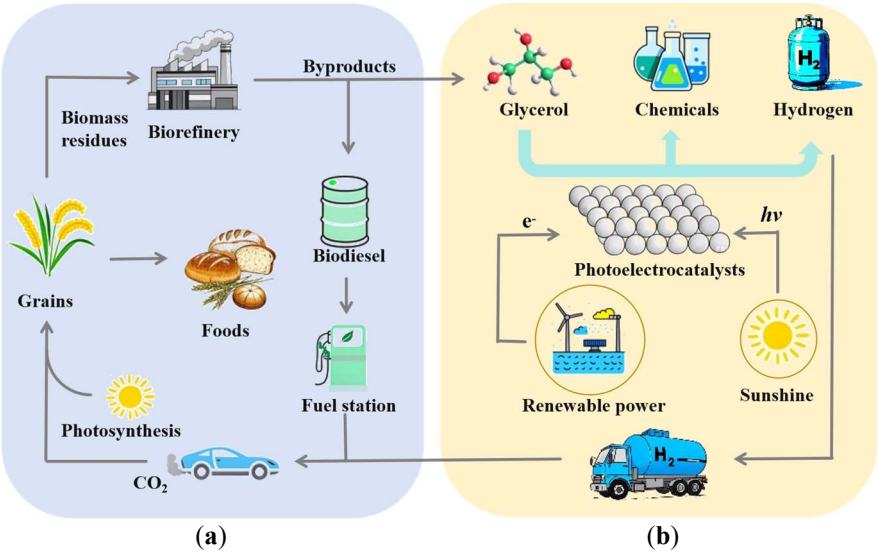

Figure 1. Sustainable glycerol valorization. (**a**) Carbon cycle pathways. (**b**) Renewable powered PEC glycerol conversion coupled with hydrogen production. Drawn according to ref. [5].

2. Mechanism of PEC Glycerol Oxidation

The major pathways and products of PEC glycerol oxidation can be summarized in Figure 2. Generally, PEC glycerol oxidation involves oxidation of the terminal or middle C–OH/C=O bond and C–C oxidative cleavage. For the formation of C3 products, only oxidation of the terminal or middle C–OH/C=O bond occurs, while further C–C oxidative cleavage occurs for the formation of C2 and C1 products. During the glycerol oxidation process, the thermodynamic energy barriers for C–H bond activation and secondary C–H bond breaking are relatively similar, resulting in inevitably competitive reactions [5].

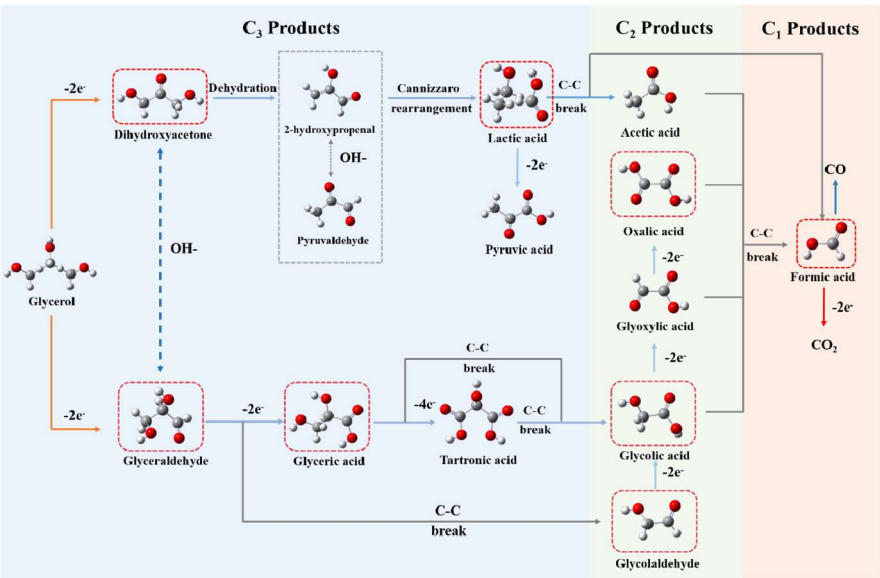

Figure 2. The major pathways and products of PEC glycerol oxidation. Drawn according to ref. [5].

In a PEC system (Figure 3), the photogenerated electrons near the photoanode under irradiation are transferred through an external circuit to the counter electrode to reduce water to produce hydrogen, while the Photogenerated holes left participate in the oxidation of glycerol. Therefore, the properties of the photoanode catalyst play a crucial role in determining the cleavage sites of the C–C bond and C–OH/C=O bond, thus significantly affecting the selectivity of glycerol oxidation. Typical semiconductors such as TiO_2 [3,12], WO_3 [13,14], $BiVO_4$ [15,16], ZnO [17], Ta_3N_5 [18], and α-Fe_2O_3 [19] have been examined for PEC glycerol oxidation with different main products [20].

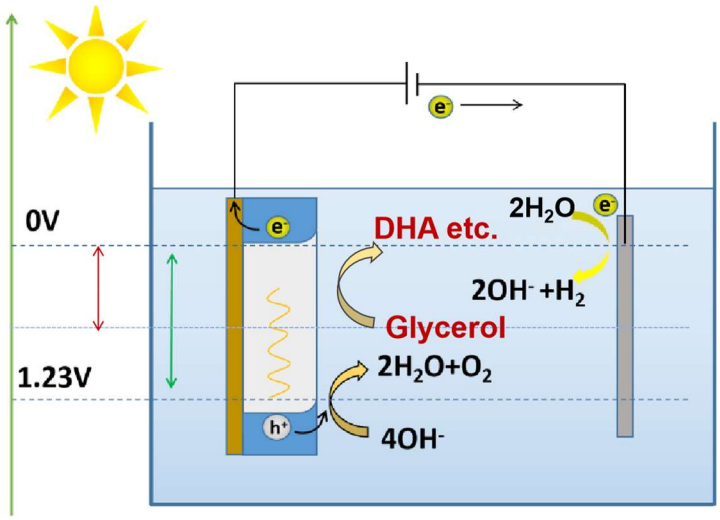

Figure 3. Typical PEC reaction setup.

3. Improving the Selectivity and Productivity of PEC Glycerol Oxidation

Glycerol oxidation reaction involves complex multielectron transfer processes across multiple reaction pathways, leading to a diverse and intricate product distribution and a low selectivity for targeted GOR products. Selective PEC glycerol oxidation aims to selectively oxidize glycerol into value-added liquid products while simultaneously generating high purity and large quantities of H_2, which relies not only on the catalyst nature but also on how the reaction is conducted. Great efforts such as elemental doping, interface engineering, and surface modification have been made to improve the product selectivity and yield in GOR from various perspectives, such as enhancing adsorption properties, improving electron conduction properties, adjusting the energy band structure, and increasing light absorption [14,21–24]. As displayed in Figure 4, the catalyst nature and the reaction conditions, such as the concentration of reactants, the type and pH of electrolyte used, and the mass-transfer conditions, can synergistically influence the overall performance of glycerol oxidation [25,26]. In the following, we will introduce the recent progress in view of the product types, considering these factors mainly focusing on the most potential $BiVO_4$-based, TiO_2-based, and WO_3-based photoanodes.

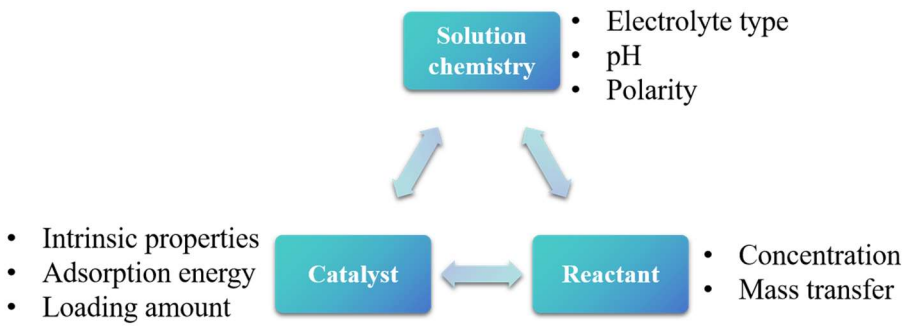

Figure 4. Dominant influencing factors on glycerol oxidation performance [26].

3.1. $BiVO_4$-Based Photoanodes

Among various semiconductors, bismuth-based photoanodes are considered one of the most potential photoanode materials for selective PEC oxidation of glycerol. Table 1 shows the representative $BiVO_4$-based photoanodes for the PEC glycerol oxidation. The GOR products based on single $BiVO_4$ photoanodes can be dominated either by FA or by DHA. The specific dominant product depends on the type of electrolyte solution and its pH value, as well as the electronic structure of the catalyst surface.

Table 1. List of the representative $BiVO_4$-based photoanodes for the PEC glycerol oxidation.

Photoanode	Electrolyte	Main Product	Production Rate ($mmol \cdot m^{-2} \cdot h^{-1}$)	Selectivity (%)	H_2 Production Rate ($mmol \cdot m^{-2} \cdot h^{-1}$)	Ref.
$WO_3/BiVO_4/Bi$	0.5 M Na_2SO_4 (pH = 2)	DHA	192.69	60.60	328.8	[27]
$BiVO_4$/CoV-LDHs/Ag	0.5 M Na_2SO_4 (pH = 2)	FA	54	-	123.5	[21]
$BiVO_4$	0.1 M HNO_3	FA	436.45	78.1	333	[26]
BVO/TANF(Ni^{2+}/Fe^{2+})	0.1 M Na_2SO_4 (pH = 2)	FA	573	85	500	[28]
B:$NiCoO_x/BiVO_4$	0.5 M Na_2SO_4 (pH = 2)	FA + DHA	360.3 (FA)+ 228.4 (DHA)	-	1290	[29]
$BiVO_4$/CoOx/Au	0.5 M Na_2SO_4 (pH = 2)	DHA	339.74	60	-	[30]
porous $BiVO_4$	0.5 M Na_2SO_4 (pH = 2)	DHA	325.2	53.70	-	[31]
Ta-$BiVO_4/WO_3$	0.1 M Na_2SO_4 (with acetone)	DHA	-	100	130	[7]

Huang et al. reported GOR over $BiVO_4$ photoanode with glycerol being oxidized to valuable products of 15% dihydroxyacetone (DHA) and 85% formic acid in a mixed electrolyte solution composed of 0.1 M $Na_2B_4O_7$ (pH = 9.4) and 0.1 M glycerol under 1 sun illumination [15]. Liu et al. [32] investigated the effect of electrolyte pH on the selectivity and production rate of PEC GOR over porous $BiVO_4$ nanoarrays (Figure 5a,b). The selectivity and production rate of DHA reaches ~50% and 200 $mmol \cdot m^{-2} \cdot h^{-1}$ at 1.2 V *vs*. RHE at pH = 2 from ~ 30% with pH = 5 and 7, respectively. The results demonstrate that lower pH enables easier glycerol adsorption on $BiVO_4$, which results in an easier charge transfer and enhanced catalysis to PEC glycerol conversion when reaction pH is decreased. Besides, an acidic environment can also suppress the reaction towards acid products, which leads to a high selectivity of DHA.

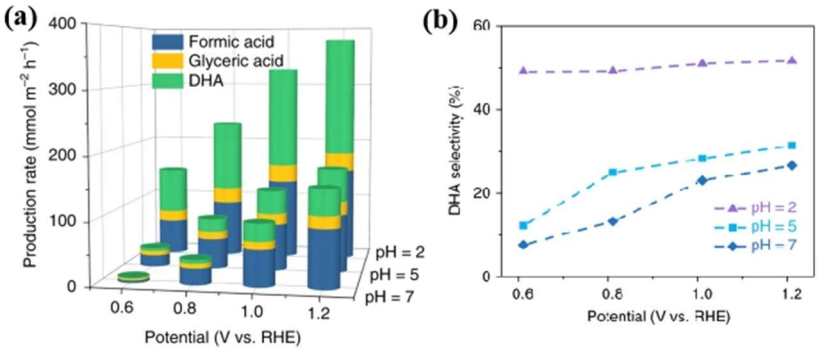

Figure 5. (**a**,**b**) Effect of pH value on the PEC glycerol performance of $BiVO_4$ potoanode. (**a**) Rates of GOR products at different pH; (**b**) Selectivity of DHA at different pH. Reprinted with permission from [32]. Copyright 2019, Springer Nature.

Further, Cui et al. [26] investigated the effect of electrolyte type on the performance of PEC glycerol oxidation over $BiVO_4$ photoanode. It is found that the photocurrent density in H_2SO_4 is obviously higher than that in HNO_3. The total production rate increased with applied potential, and the yield in HNO_3 consistently exceeded that in H_2SO_4. At 1.4 V *vs.* RHE, the production rate of FA rose from 305.75 $mmol \cdot m^{-2} \cdot h^{-1}$ in H_2SO_4 to 436.45 $mmol \cdot m^{-2} \cdot h^{-1}$ in HNO_3, indicating that NO_3^- anions promote FA production. Additionally, a high selectivity for FA of 78.1% was achieved in HNO_3. The results highlight the significant influence of anions on the PEC performance.

After deposition of FeOOH cocatalyst, highly selective conversion of glycerol into valuable GLD is obtained over $BiVO_4$/FeOOH with a thin amorphous layer of FeOOH onto the surface of $BiVO_4$. The GLD production rate reached 709 $mmol \cdot m^{-2} \cdot h^{-1}$ with a selectivity of 63.3% using a Na_2SO_4 solution under AM1.5G (100 $mW \cdot m^{-2}$) light intensity at 1.23 V *vs.* RHE [33].

It is reported that the bismuth (Bi) atom exhibits a heightened electrostatic adsorption capacity for the secondary hydroxyl of glycerol [27]. Lu et al. [34] synthesized Bi-rich $BiVO_{4-x}$ and investigated its PEC GOR performance (Figure 6a,b). The results demonstrate that the photocurrent density of Bi-rich $BiVO_{4-x}$ photoanode in GOR increases from 1.42 to 4.26 $mA \cdot cm^{-2}$ at 1.23 V *vs.* RHE under AM 1.5 G illumination, accompanied by a selectivity increase of DHA product from 54% to 80.3%, finally achieving a DHA conversion of 361.9 $mmol \cdot m^{-2} \cdot h^{-1}$ (Figure 6c). The high selectivity for DHA can be ascribed to the Bi-rich surface, which is favorable for secondary hydroxyl adsorption for glycerol (Figure

6d). The high conversion rate is due to the additionally introduced oxygen vacancies (Ov), which enhance the interaction frequency of Bi atoms at the interface, leading to an improvement in surface charge transport efficiency.

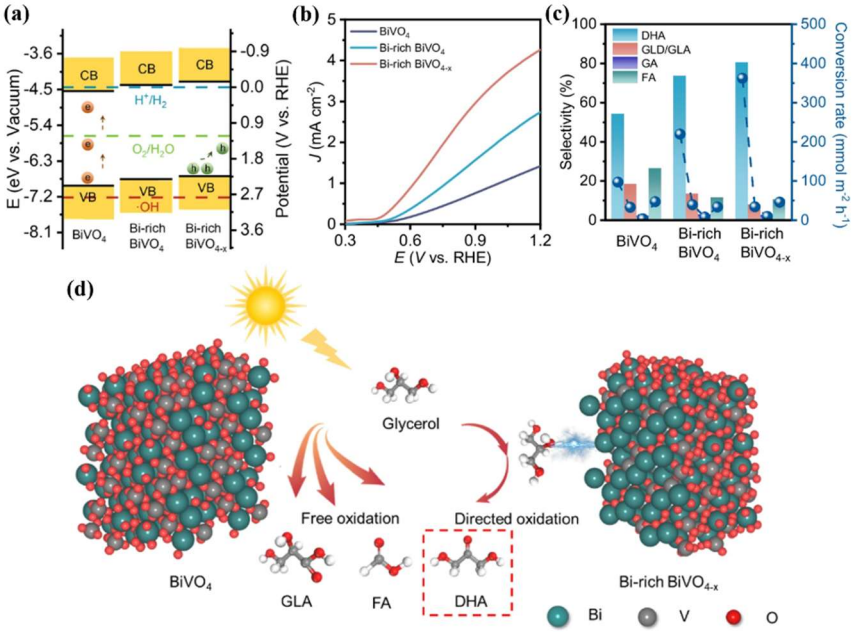

Figure 6. (**a**–**c**) PEC GOR performance and charge behavior. (**d**) Schematic illustration of the PEC GOR to DHA over Bi-rich $BiVO_{4-x}$ photoanode. Reprinted with permission from [34]. Copyright 2024, Springer Nature.

On the other hand, Han et al. [28] reported that the $BiVO_4$ photoanode modified by phenolic ligands (tannic acid, TA) and Ni^{2+}/Fe^{2+} ions (denoted TANF) (Figure 7a–i) shows a high production rate of 573 $mmol \cdot m^{-2} \cdot h^{-1}$ toward FA with high selectivity of 85% in a 0.1 M Na_2SO_4/H_2SO_4 electrolyte (pH = 2) (Figure 7j–k).

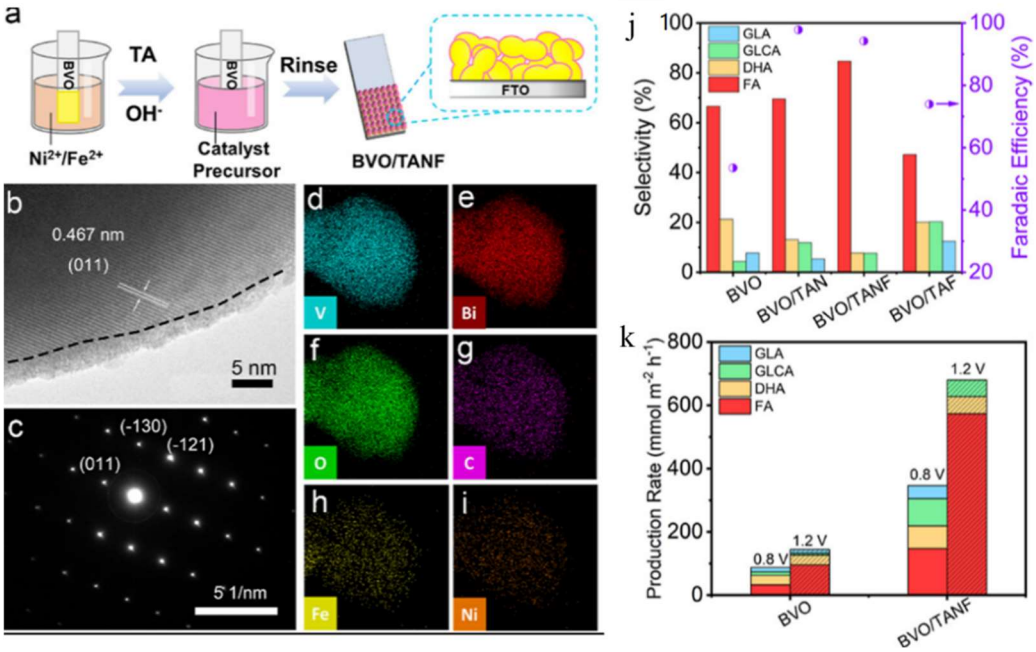

Figure 7. (**a**) Schematic illustration of the synthesis of the BVO (porous $BiVO_4$)/TANF film. (**b**–**i**) Morphology of the BVO/TANF film. (**j**,**k**) The PEC GOR performance of BVO/TANF film. (**j**) Selectivity and faradaic efficiency of GOR products; (**k**) Production rates of GOR products. Reprinted with permission from [34]. Copyright 2023, American Chemical Society.

Therefore, we can conclude that the surface structure, the pH, the type of electrolyte, and the electronic structure of the catalyst surface can significantly influence the PEC GOR performance of $BiVO_4$-based photoanodes.

3.2. TiO_2-Based Photoanodes

TiO_2 is also one of the prominent semiconductors frequently explored in PEC energy conversions. Table 2 shows the representative TiO_2-based photoanodes for the PEC glycerol oxidation. Similarly, the GOR products based on single TiO_2 photoanodes can be dominated either by FA or by DHA. The specific dominant product also depends on the type of electrolyte solution and its pH value, as well as the electronic structure of the catalyst surface.

Table 2. List of the representative TiO_2-based photoanodes for the PEC glycerol oxidation.

Photoanode	Electrolyte	Main Product	Production Rate ($mmol \cdot m^{-2} \cdot h^{-1}$)	Selectivity (%)	H_2 Production Rate ($mmol \cdot m^{-2} \cdot h^{-1}$)	Ref.
Bi_2O_3/TiO_2	0.5 M Na_2SO_4 (pH = 2)	DHA	115	75.4	140	[12]
WO_3 NSs/TiO_2 NRs	0.1 M Na_2SO_4	GLD	319	61	33300	[23]
TiO_2(N-C)/CPB/TiO_2	0.1 M Na_2SO_4 (pH=2)	DHA	167	52	-	[35]
TiO_2 nanotubes-100	0.5 M Na_2SO_4 (pH = 2)	FA	43	59.0	-	[8]
TiO_2 nanotubes-50	0.5 M Na_2SO_4 (pH = 2)	GLD	56	60.70	-	[8]
Co-LDH(6 h)/TiO_2	0.1 M Na_2SO_4 (pH = 7)	DHA	-	48	20.35	[36]
Ag@LDH@TiO_2	0.5 M Na_2SO_4 (pH=7)	DHA	315	72	-	[3]
CdS/TiO_2	1 M KOH (pH = 13)	FA	367.6	49.84	1574.5	[37]
IrO_2/CdS/TiO_2	1 M KOH (pH = 13)	FA	551.4	53.22	2345.2	[37]

Lu et al. [8] investigated the microscale fluid effect on the selectivity of the GOR products over TiO_2 nanotube photoanode. They provided an alternative way to regulate the intrinsic selectivity of TiO_2 photoanode by altering the microenvironment (Figure 8). It is found that the action of microfluidics can effectively inhibit the overoxidation of glycerol due to the rapid mass transfer, which enables the quick desorption and discharge of multiple carbon products (Figure 8a). The TiO_2 nanotubes with a diameter of 50 nm show a great selectivity of 60.9% for GLD (Figure 8b,c).

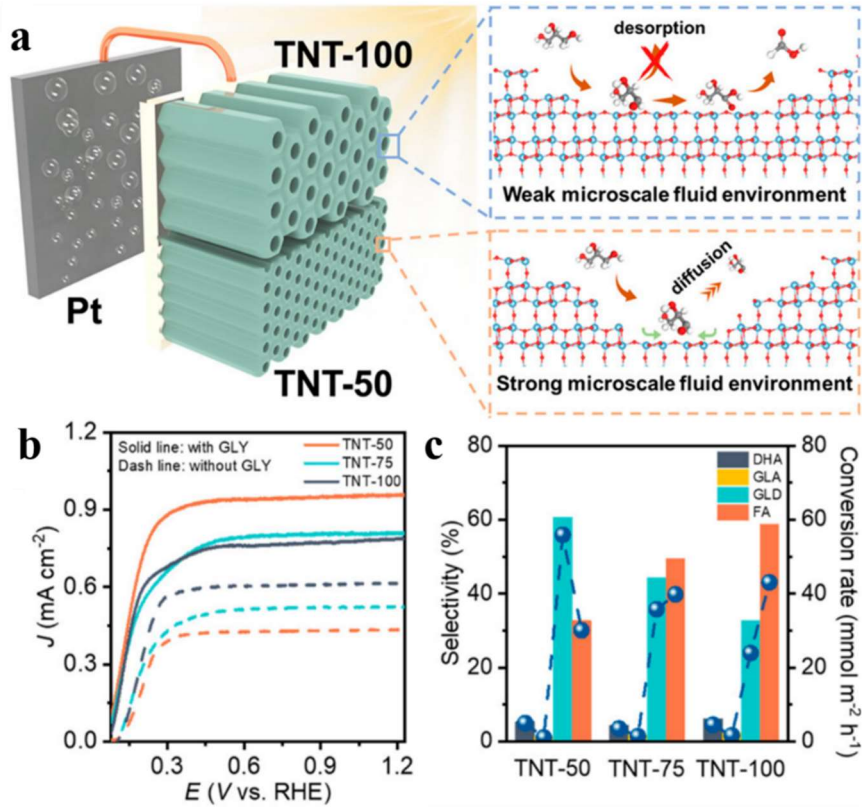

Figure 8. (**a**) Schematic diagram of the role of microscale fluid in the PEC GOR. (**b**) LSV curves of the different photoanodes in 0.5 M Na_2SO_4 (pH = 2) with and without glycerol. (**c**) GOR conversion rate and selectivity of the main products. Reprinted with permission from [8]. Copyright 2024, American Chemical Society.

As demonstrated above, the surface structure plays a crucial role in determining the selectivity of GOR. Therefore, introducing cocatalysts is expected to alter the types of GOR products formed. Duan et al. [13] designed a heterogeneous photoanode of Bi_2O_3 nanoparticles on TiO_2 nanorod arrays (Bi_2O_3/TiO_2) (Figure 9a–c). The selectivity of DHA can be maintained at ~65% under a relatively high conversion of glycerol (~50%) (Figure 9d–f). In a self-powered PEC system,

a DHA productivity of 1.04 mg·cm^{-2}·h^{-1} with >70% selectivity and a H_2 productivity of 0.32 mL·cm^{-2}·h^{-1} were achieved. The authors attribute the enhancement to the existing p−n junction between Bi_2O_3 and TiO_2, which promotes charge transfer and thus guarantees high photocurrent density, and the introduced Bi_2O_3, which prefers to interact with the middle hydroxyl of glycerol, facilitating the high selectivity of DHA.

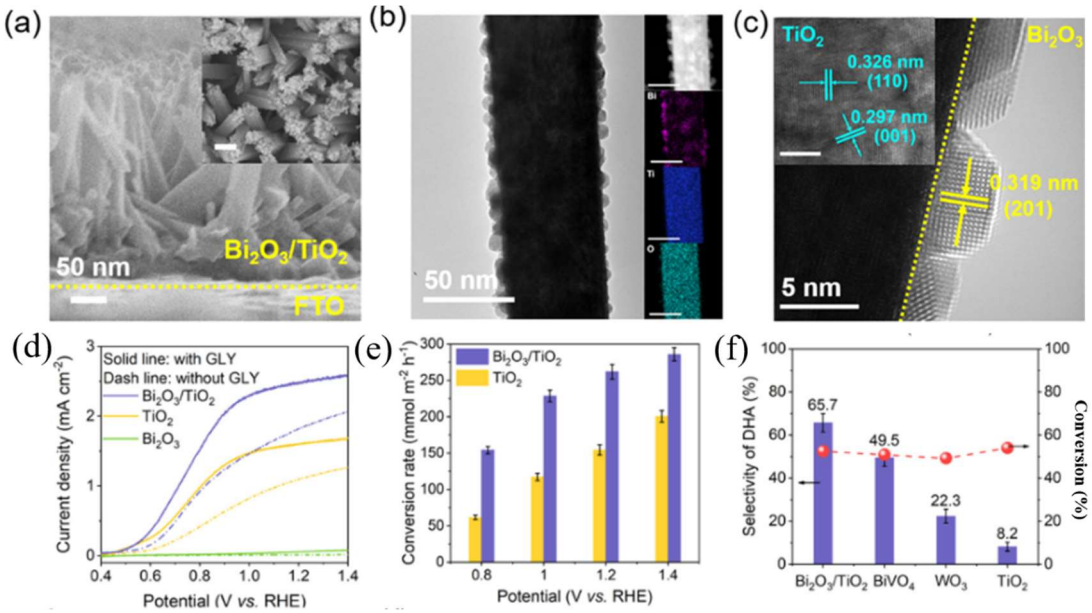

Figure 9. (**a**–**c**) Morphology of Bi_2O_3/TiO_2. (**a**) SEM images; (**b**) STEM-EDS mapping results of a single Bi_2O_3/TiO_2 nanorod; (**c**) HRTEM images of a representative region. (**d**–**f**) Performance of the Bi_2O_3/TiO_2 photoanode for PEC glycerol oxidation. (**d**) LSV curves; (**e**) Conversion rate of glycerol (GLY) at different potentials; (**f**) Selectivity of DHA over different photoanodes. Reprinted with permission from [13]. Copyright 2022, American Chemical Society.

Li et al. [23] investigated the effect of loading of WO_3 nanosheets on TiO_2 nanorod arrays on the PEC glycerol conversion performance. The optimized composite photoanode achieved a selectivity of 61% for GLD and 31% for DHA at 1.23 V *vs.* RHE in 0.1 M Na_2SO_4 and 0.05 M glycerol (pH = 7) with formation rates of 319 and 160 mmol·m^{-2}·h^{-1}, respectively. The results demonstrate that single TiO_2 tends to over-oxidize glycerol into lower-value products, and the selectivity of WO_3/TiO_2 towards higher-value products (GLD and DHA) is significantly enhanced after loading of WO_3 due to its good adsorption of glycerol and desorption of GLD and DHA. In addition, the selectivity for GLD and DHA remains almost unchanged over a 10 h period, suggesting good stability.

Liu et al. [3] reported the Ag nanoparticle-supported layered double hydroxide (LDH) nanosheets on TiO_2 (denoted Ag@LDH@TiO_2) for the glycerol selective oxidation to DHA (Figure 10a). The Ag@LDH@TiO_2 photoanode exhibited a DHA selectivity of 72% with a production rate of ~310 mmol·m^{-2}·h^{-1} at 1.2 V *vs.* RHE, which is obviously higher than that of pure TiO_2 (23.5%, less than 200 mmol·m^{-2}·h^{-1}) (Figure 10b,c). This is due to the fact that the LDHs and Ag nanoparticles both enhanced the selective adsorption of secondary hydroxyl of glycerol, leading to its selective oxidation to DHA.

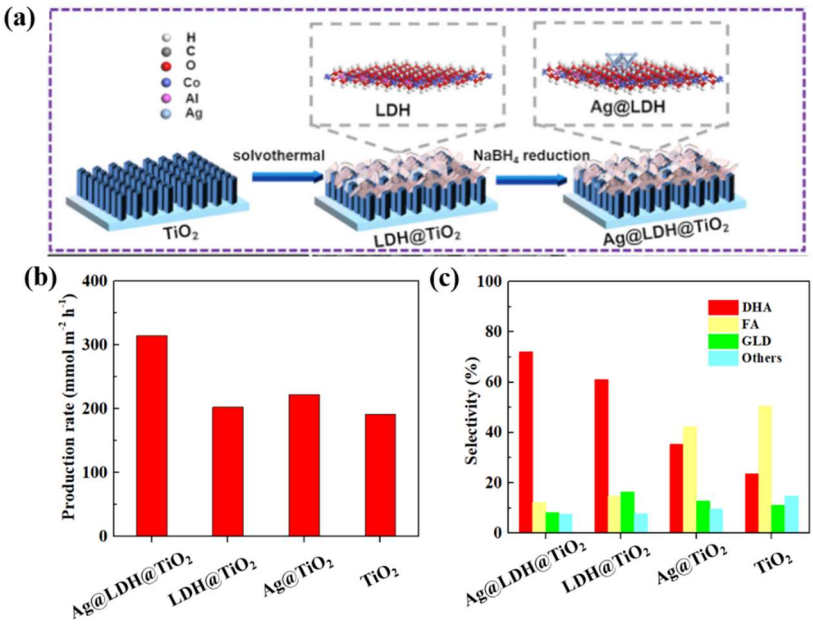

Figure 10. (**a**) Synthetic process of the Ag@LDH@TiO_2 photoanode. (**b**,**c**) GOR performance. (**b**) Production rates and (**c**) selectivity of GOR products. Reprinted with permission from [3]. Copyright 2022, American Chemical Society.

Though the selectivity of TiO_2 can be significantly modified by introducing cocatalysts, its PEC activity still falls short of meeting the requirements for practical applications. CdS is a typical semiconductor with a narrow band gap and high absorption coefficient, which has been widely investigated in PEC water splitting by constructing TiO_2/CdS heterojunction. However, the hole-induced photocorrosion of CdS brings big trouble due to poor stability. Jiang et al. [37] investigated the TiO_2/CdS heterojunction photoanode in the application of GOR (Figure 11a,b). As shown in Figure 11c, the photocurrent density of the optimized TiO_2/CdS photoanode is 18.8 mA cm^{-2} (1.23 V *vs.* RHE), which is about 10.6 times higher than that of the pristine TiO_2. The TiO_2/CdS photoanode shows a high selectivity of 49.84% for FA with a production rate ~1574.5 $mmol \cdot m^{-2} \cdot h^{-1}$. After loading IrO_2 nanoparticles, the selectivity for FA is enhanced to 53.22%, with the production rate reaching 2345.2 $mmol \cdot cm^{-2} \cdot h^{-1}$ due to the improved stability (Figure 11d). This is the highest production rate ever reported. The enhanced PEC performance and stability of the TiO_2/CdS/IrO_2 photoanode can be ascribed to the greatly enhanced electrode/electrolyte interfacial carrier injection efficiency caused by the fast glycerol oxidation dynamics and intimate contact.

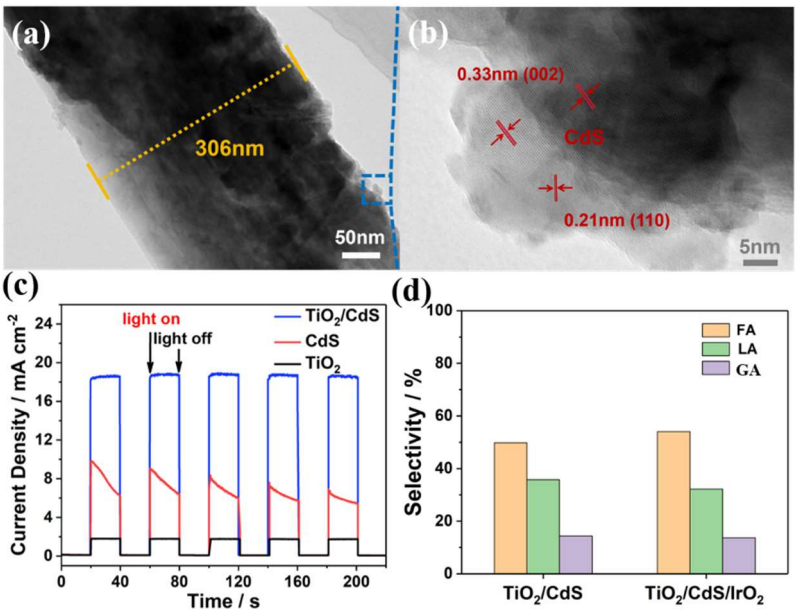

Figure 11. (**a**) TEM and (**b**) HRTEM images of TiO_2/CdS photoanode. (**c**) Transient photoresponse at 1.23 V *vs.* RHE in 1 M KOH containing 0.3 M glycerol. (**d**) Selectivity of GOR products over TiO_2/CdS and TiO_2/CdS/IrO_2 photoanodes . Reproduced from Ref. [37] with permission from the Royal Society of Chemistry.

3.3. WO_3-Based Photoanodes

WO_3 stands out as another prominent semiconductor frequently explored in PEC glycerol oxidation for C3 products. Table 3 shows the representative WO_3-based photoanodes for the PEC glycerol oxidation.

Table 3. List of the representative WO_3-based photoanodes for the PEC glycerol oxidation.

Photoanode	Electrolyte	Main Product	Production Rate ($mmol \cdot m^{-2} \cdot h^{-1}$)	Selectivity (%)	H_2 Production Rate ($mmol \cdot m^{-2} \cdot h^{-1}$)	Ref.
(002) WO_3	0.1 M Na_2SO_4 (pH = 2)	GA	25	75	-	[38]
(202) WO_3	0.1 M Na_2SO_4 (pH = 2)	GLD	462	80	-	[13]
(200) WO_3	0.1 M Na_2SO_4 (pH = 2)	GLD	173	71	-	[13]
Bi-MOFs/WO_3	0.1 M Na_2SO_4 (pH = 2)	GLD	420	93.6	433	[39]
Pt-SA/WO_x	0.5 M Na_2SO_4 (pH = 2)	DHA	297.3	60.2	203.2	[40]

For example, Yu et al. [41] reported the PEC behavior of monoclinic WO_3 in oxidizing glycerol to higher-value C3 products, such as DHA and glyceraldehyde. The monoclinic WO_3 showed a high and stable selectivity for glyceraldehyde and DHA, with selectivity between 87 and 95% within a potential range of 0–1.5 V *vs.* Ag/AgCl under ambient conditions and near-neutral pH, outperforming those of commercially available WO_3/TiO_2 (DTW5) catalyst. The high selectivity of the WO_3 photoanode, as well as DTW5 for C3 compounds and, specifically, for glyceraldehyde, is likely influenced by the strong acidity of WO_3, which can enhance the desorption of these products from the catalyst surface, as previously reported on glycerol oxidation and dehydrogenation reactions. Besides, the high selectivity towards primary C3 products of WO_3 is also linked to its high activity for the PEC oxygen evolution, which could promote the direct glycerol oxidation mechanism.

It is reported that the exposed facets determine the surface structure of a photocatalyst and, therefore its physicochemical properties and photocatalytic activities [42]. Xiao et al. [38] reported the selective PEC glycerol oxidation to glyceric acid (GA) on (002) facets exposed WO_3 nanosheets in 0.5 M H_2SO_4 solution (Figure 12a,b). As shown in Figure 12c,d, GA is the primary product under all applied potentials with the selectivity approaching 75% on WO_3 nanosheet photoanode with preferentially exposed (002) facets (002-W) at 0.7 V_{RHE}, and 70% on WO_3 nanorod photoanode with preferentially exposed (200) facets (200-W) at 1.0 V_{RHE}. The 002-W shows higher PEC oxidation activity than the commonly studied 200-W, achieving GA production rate of 32.3 $mmol \cdot m^{-2} \cdot h^{-1}$ at 0.9 V_{RHE} under AM 1.5G illumination. The total selectivity of C3 products (GA + DHA) reaches as high as 96% over 002-W. It is disclosed that the abundant surface states on (002) facets of WO_3 can dramatically enhance charge separation and increase the carrier lifetime. Moreover, the 002-W exhibits a lower energy barrier for glycerol oxidation to GA as compared to 200-W [43].

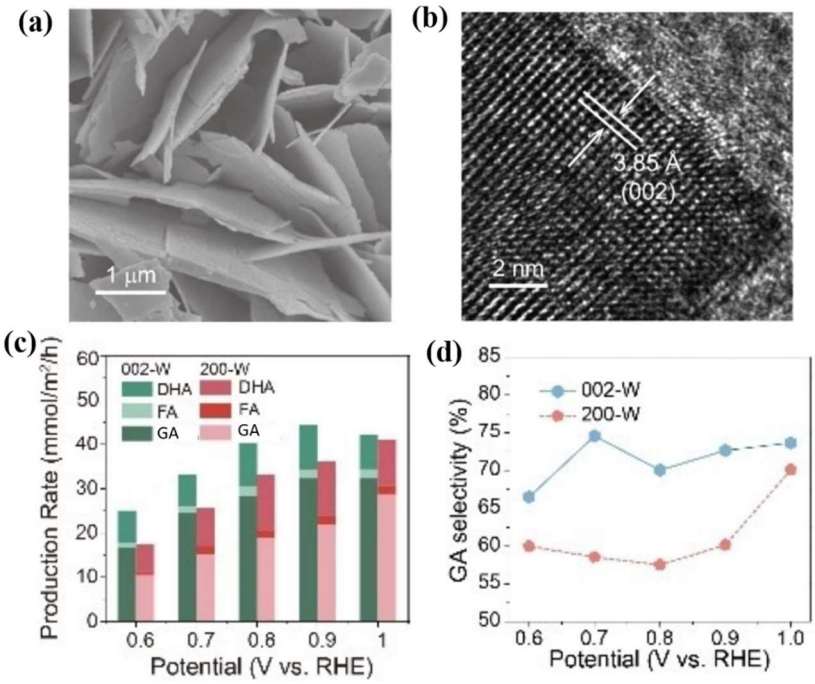

Figure 12. (**a**,**b**) Morphology of (002) WO_3 (002-W). (**a**) SEM image, (**b**) HRTEM image. (**c**,**d**) PEC glycerol oxidation performance in 0.5 M H_2SO_4 containing 0.1 M glycerol. (**c**) PEC production rates of GOR products on 002-W and 200-W in 1 h.

(**d**) Selectivity of GA on 002-W and 200-W in 6 h. Reproduced with permission. [38] Copyright 2024, Wiley VCH Weinheim.

The comparison between the {202} facets and the commonly studied {200} facets of WO_3 was also investigated (Figure 13a,b) [13]. As shown in Figure 13c–e, the WO_3 {202} photoanode displays a high 80% selectivity to glyceraldehyde (GLD) with a production rate of 462 $mmol \cdot m^{-2} \cdot h^{-1}$, about 2.7 times higher than that of WO_3 {200} photoanode (173 $mmol \cdot m^{-2} \cdot h^{-1}$) with a selectivity of 71%. The enhanced PEC performance for GOR can be attributed to the fact that the WO_3 predominated with the {202} facet has a lower band gap, higher carrier concentration, and facilitated interface charge transfer compared with the WO_3 photoanode predominated with the {200} facet. Furthermore, the {202} crystal facet is beneficial to the adsorption and activation of glycerol via the terminal hydroxyl groups as well as the desorption of glyceraldehyde.

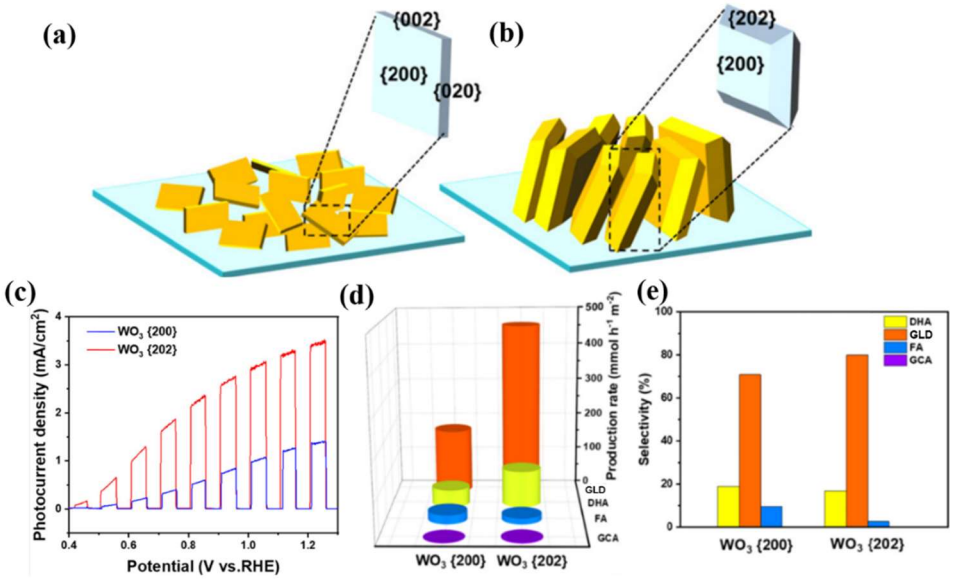

Figure 13. (**a**) WO_3 {200} and (**b**) WO_3 {202} photoanode. (**c**) Chopped photocurrent density–potential curves over, (**d**) production rate of and (**e**) selectivity to oxidation products over WO_3 {200} and WO_3 {202} photoanodes at 1.2 V *vs.* RHE in 0.1 M Na_2SO_4 with 1 M glycerol (pH = 2). Reprinted with permission from [13]. Copyright (2022) American Chemical Society.

Feng et al. [40] investigated the effect of Pt single atom (SA) doping and oxygen vacancies on the PEC glycerol oxidation performance of WO_3 photoanode (Figure 14a). The results demonstrate that the coupled Pt-SA/WO_x photoanode has a highest photocurrent density of 2.85 $mA \cdot cm^{-2}$ at 1.2 V versus RHE with a DHA selectivity of 60.2%, higher than that of WO_3 (48.6%) and WO_x with rich oxygen vacancies (55.5%) (Figure 14b,c). The enhanced PEC activity and DHA selectivity are ascribed to the regulated band structure, built-in electric field, and surface charge density of Pt-SA/WO_x.

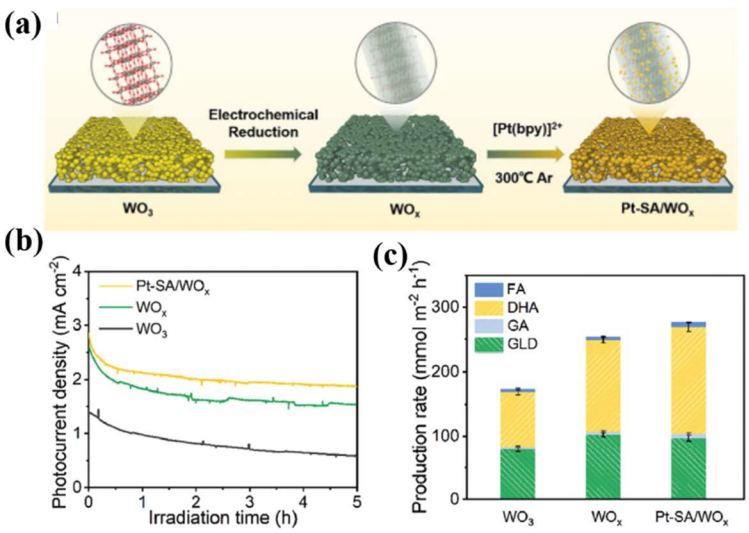

Figure 14. (**a**) Fabrication process and structural characterizations of Pt-SA/WO_x. (**b**,**c**) The PEC glycerol performance of the

photoanodes in 0.5 M Na_2SO_4 mixed with 0.1 M glycerol with pH = 2. (**b**) *J-t* stability tests. (**c**) PEC production rate of oxidation products. Reproduced with permission. [40] Copyright 2024, Wiley VCH Weinheim.

As mentioned above, the semiconductor surface chemical structures play a key role in the inherent thermodynamic adsorption of glycerol [24,44,45]. Consequently, even minor changes in the surface structure can significantly affect the adsorption behavior of semiconductors to the electrolyte and, finally, the selectivity of the PEC upgrading anode reaction[29,46]. Therefore, facet manipulation and cocatalyst decoration are considered promising approaches for enhancing the selectivity of GOR products in the future [47–49].

4. Conclusions

In summary, glycerol oxidation instead of water oxidation can greatly reduce hydrogen overpotential and accelerate hydrogen production. Meanwhile, glycerol oxidation will produce high value-added chemicals, which will reduce the cost of hydrogen production, making the price of hydrogen competitive with other methods of hydrogen production. Summarized from recent work, we found that $BiVO_4$ and WO_3-based photoanodes have great potential applications for generating C3 products, while TiO_2-based photoanodes tend to produce C1 products. It should be noted that the surface structure plays a critical role in the PEC GOR performance, including selectivity and production rates. To improve the selectivity of upgrading anode reactions, most recent research on upgrading PEC anode reactions follows these two strategies: (1) modifying the surface chemical structure of anode materials to adjust their thermodynamic properties and carriers concentration such as facet manipulation, doping, and defect engineering, and (2) decorating the anode materials with cocatalysts to adjust the surface properties, charge separation and light absorption. Indeed, to develop high efficient PEC glycerol photoanode with high selectivity towards one of the high value-added products, various strategies should be combined based on the structure–performance relationships.

Ethics Statement

Not applicable.

Informed Consent Statement

Not applicable.

Data Availability Statement

The statement is required for all original articles which informs readers about the accessibility of research data linked to a paper and outlines the terms under which the data can be obtained.

Funding

This work was supported by the National Natural Science Foundation of China (NSFC) (Grant No. 51972318).

Declaration of Competing Interest

The author declares that he/she has no known competing financial interests or personal relationships that could have appeared to influence the work reported in this paper.

References

1. Sendeku MG, Shifa TA, Dajan FT, Ibrahim KB, Wu B, Yang Y, et al. Frontiers in photoelectrochemical catalysis: A focus on valuable product synthesis. *Adv. Mater.* **2024**, *36*, 2308101.
2. Yu J, González-Cobos J, Dappozze F, Grimaldos-Osorio N, Vernoux P, Caravaca A, et al. First PEM photoelectrolyser for the simultaneous selective glycerol valorization into value-added chemicals and hydrogen generation. *Appl. Catal. B Environ. Energy* **2023**, *327*, 122465.
3. Liu Y, Wang M, Zhang B, Yan D, Xiang X. Mediating the oxidizing capability of surface-bound hydroxyl radicals produced by photoelectrochemical water oxidation to convert glycerol into dihydroxyacetone. *ACS Catal.* **2022**, *12*, 6946–6957.
4. Chuang PC, Lin CY, Ye ST, Lai YH. Earth-abundant $CuWO_4$ as a versatile platform for photoelectrochemical valorization of soluble biomass under benign conditions. *Small* **2024**, *20*, 2404478.
5. Ma GQ, Jiang N, Song DD, Qiao B, Xu Z, Zhao S, et al. Efficient strategies for designing photoanodes toward selective photoelectrochemical glycerol upgrading: a review. *J. Mater. Chem. A* **2025**, *13*, 889–917.

6. Hou Y, Xia C, Wang S, Lei Q, Li Y, Xu H, et al. Beyond water splitting: Developing economic friendly photoelectrochemical value-added reactions for green solar-to-chemical energy conversions. *Korean J. Chem. Eng.* **2024**, 1–24.
7. Tateno H, Chen S-Y, Miseki Y, Nakajima T, Mochizuki T, Sayama K. Photoelectrochemical oxidation of glycerol to dihydroxyacetone over an acid-resistant Ta:$BiVO_4$ photoanode. *ACS Sustain. Chem. Eng.* **2022**, *10*, 7586–7594.
8. Lu Y, Liu T-K, Lin C, Kim KH, Kim E, Yang Y, et al. Nanoconfinement enables photoelectrochemical selective oxidation of glycerol via the microscale fluid effect. *Nano Lett.* **2024**, *24*, 4633–4640.
9. Miao Y, Li Z, Shao MY. Photoelectrochemical glycerol oxidation coupled with hydrogen production. *ChemCatChem* **2024**, *16*, e202301321.
10. Shi Q, Duan H. Recent progress in photoelectrocatalysis beyond water oxidation. *Chem. Catal.* **2022**, *2*, 3471–3496.
11. Kumar M, Meena B, Yu A, Sun C, Challapalli S. Advancements in catalysts for glycerol oxidation via photo-/electrocatalysis: a comprehensive review of recent developments. *Green Chem*. **2023**, *25*, 8411–8443.
12. Luo L, Chen W, Xu S-M, Yang J, Li M, Zhou H, et al. Selective photoelectrocatalytic glycerol oxidation to dihydroxyacetone via enhanced middle hydroxyl adsorption over a Bi_2O_3-incorporated catalyst. *J. Am. Chem. Soc.* **2022**, *144*, 7720–7730.
13. Ouyang J, Liu X, Wang B-H, Pan J-B, Shen S, Chen L, et al. WO_3 photoanode with predominant exposure of {202} facets for enhanced selective oxidation of glycerol to glyceraldehyde. *ACS Appl. Mater. Interfaces* **2022**, *14*, 23536–23545.
14. Peerakiatkhajohn P, Yun J-H, Butburee T, Lyu M, Takoon C, Thaweesak S. Dual functional WO_3/$BiVO_4$ heterostructures for efficient photoelectrochemical water splitting and glycerol degradation. *RSC Adv.* **2023**, *13*, 18974–18982.
15. Huang L-W, Vo T-G, Chiang C-Y. Converting glycerol aqueous solution to hydrogen energy and dihydroxyacetone by the $BiVO_4$ photoelectrochemical cell. *Electrochim. Acta* **2019**, *322*, 134725.
16. Wu Y-H, Kuznetsov DA, Pflug NC, Fedorov A, Müller CR. Solar-driven valorisation of glycerol on $BiVO_4$ photoanodes: effect of co-catalyst and reaction media on reaction selectivity. *J. Mater. Chem. A* **2021**, *9*, 6252–6260.
17. Tan L, Sun Y, Yang C, Zhang B, Deng K, Cao X, et al. ZnO/Fe-thioporphyrazine composites as efficient photocatalysts for oxidation of glycerol to value-added C3 products in water. *Mol. Catal.* **2023**, *537*, 112972.
18. Wang Q, Ma X, Wu P, Li B, Zhang L, Shi J. CoNiFe-LDHs decorated Ta_3N_5 nanotube array photoanode for remarkably enhanced photoelectrochemical glycerol conversion coupled with hydrogen generation. *Nano Energy* **2021**, *89*, 106326.
19. Chong R, Wang B, Li D, Chang Z, Zhang L. Enhanced photoelectrochemical activity of Nickel-phosphate decorated phosphate-Fe_2O_3 photoanode for glycerol-based fuel cell. *Sol. Energy Mater Sol. Cells* **2017**, *160*, 287–293.
20. Li J, Wu N. Semiconductor-based photocatalysts and photoelectrochemical cells for solar fuel generation: a review. *Catal. Sci. Technol*. **2015**, *5*, 1360–1384.
21. Xie Z, Liu X, Jia P, Zou Y, Jiang J. Facile construction of a $BiVO_4$/CoV-LDHs/Ag photoanode for enhanced photo-electrocatalytic glycerol oxidation and hydrogen evolution. *Energy Adv.* **2023**, *2*, 1366–1374.
22. Pecoraro CM, Wu S, Santamaria M, Schmuki P. Bandgap engineering of TiO_2 for enhanced selectivity in photoelectrochemical glycerol oxidation. *Adv. Mater. Interfaces* **2025**, *12*, 2400583.
23. Li X, Wang J, Wei A, Li X, Zhang W, Liu Y. Achieving high selectivity in photoelectrochemical oxidation of glycerol on WO_3 nanosheets coupled with TiO_2 nanorods arrays. *Sep. Purif. Technol.* **2024**, *332*, 125779.
24. Liu Y, Zhang B, Yan D, Xiang X. Recent advances in the selective oxidation of glycerol to value-added chemicals via photocatalysis/photoelectrocatalysis. *Green Chem*. **2024**, *26*, 2505–2524.
25. Kuo H. H, Vo T. G, Hsu Y. J. From sunlight to valuable molecules: A journey through photocatalytic and photoelectrochemical glycerol oxidation towards valuable chemical products. *J. Photochem. Photobiol. C* **2024**, *58*, 100649.
26. Cui J-Y, Li T-T, Yin Z-H, Chen L, Wang J-J. Remarkably enhanced acidic photoelectrochemical glycerol oxidation achieving the theoretical maximum photocurrent of $BiVO_4$ through anion modulation. *Chem. Eng. J.* **2024**, *493*, 152461.
27. Feng X, Feng X, Zhang F. Enhanced photoelectrochemical oxidation of glycerol to dihydroxyacetone coupled with hydrogen generation via accelerative middle hydroxyl dehydrogenation over a Bi^0/Bi^{3+} interface of a cascade heterostructure. *J. Mater. Chem. A* **2023**, *11*, 20242–20253.
28. Han Y, Chang M, Zhao Z, Niu F, Zhang Z, Sun Z, et al. Selective valorization of glycerol to formic acid on a $BiVO_4$ photoanode through NiFe phenolic networks. *ACS Appl. Mater. Interfaces* **2023**, *15*, 11678–11690.
29. Kang Z, Zheng Y, Li H, Shen Y, Zhang W, Huang M, et al. Ultrathin B:$NiCoO_x$-modified $BiVO_4$ photoanode with abundant oxygen vacancies for photoelectrochemical glycerol conversion coupled with hydrogen production. *Chem. Eng. J.* **2024**, *499*, 156324.
30. Wang L, Chen Z, Zhao Q, Wen N, Liang S, Jiao X, et al. Modulating surface oxygen valence states via interfacial potential in $BiVO_4$/CoO_x/Au photoanode for enhanced selective photoelectrochemical oxidation of glycerol to dihydroxyacetone. *Adv. Funct. Mater.* **2024**, *34*, 2409349.
31. Lin C, Dong C, Kim S, Lu Y, Wang Y, Yu Z, et al. Photo-electrochemical glycerol conversion over a Mie Scattering effect enhanced porous $BiVO_4$ photoanode. *Adv. Mater.* **2023**, *35*, 2209955.
32. Liu D, Liu JC, Cai WZ, Ma J, Yang HB, Xiao H, et al. Selective photoelectrochemical oxidation of glycerol to high value-added dihydroxyacetone. *Nat. Commun.* **2019**, *10*, 1779.

33. Gao Q, Tian R, Niu L, Wang J, Wei A, Zhang W, et al. Improved glyceraldehyde generation through FeOOH co-catalysts-modified $BiVO_4$ featuring Bi-O-Fe active sites for photoelectrocatalytic glycerol oxidation. *J. Catal.* **2024**, *438*, 115709.
34. Lu Y, Lee BG, Lin C, Liu T-K, Wang Z, Miao J, et al. Solar-driven highly selective conversion of glycerol to dihydroxyacetone using surface atom engineered $BiVO_4$ photoanodes. *Nat. Commun.* **2024**, *15*, 5475.
35. Tang R, Wang L, Zhang Z, Yang W, Xu H, Kheradmand A, et al. Fabrication of MOFs' derivatives assisted perovskite nanocrystal on TiO_2 photoanode for photoelectrochemical glycerol oxidation with simultaneous hydrogen production. *Appl. Catal. B Environ. Energy* **2021**, *296*, 120382.
36. Niu L, Tian R, Wei A, Zhang W, Wang H, Wang J, et al. Efficient photoelectrocatalytic glycerol to dihydroxyacetone synergistic hydrogen production on Co-LDH nanowires modified TiO_2 nanorod arrays. *Sep. Purif. Technol.* **2025**, *353*, 128576.
37. Jiang CF, Ding YB, Lin JY, Sun Y, Zhou W, Zhang XY, et al. Construction of ternary TiO_2/CdS/IrO_2 heterostructure photoanodes for efficient glycerol oxidation coupled with hydrogen evolution. *Dalton Trans*. **2025**, *54*, 2460–2470.
38. Xiao YH, Wang MR, Liu D, Gao JJ, Ding J, Wang H, et al. Selective photoelectrochemical oxidation of glycerol to glyceric acid on (002) facets exposed WO_3 nanosheets. *Angew. Chem*. **2024**, *136*, e202319685.
39. Jung Y, Kim S, Choi H, Kim Y, Hwang J B, Lee D, Kim Y, Park JC, Kim DY, Lee S. Photoelectrochemical selective oxidation of glycerol to glyceraldehyde with bi-based metal–organic-framework-decorated WO_3 photoanode. *Nanomaterials* **2023**, *13*, 1690.
40. Feng XY, Sun TT, Feng XF, Yu H, Yang Y, Chen LM, et al. Single-atomic-site platinum steers middle hydroxyl selective oxidation on amorphous/crystalline homojunction for photoelectrochemical glycerol oxidation coupled with hydrogen generation. *Adv. Funct. Mater*. **2024**, *34*, 2316238.
41. Yu J, González-Cobos J, Dappozze F, López-Tenllado FJ, Hidalgo-Carrillo J, Marinas A, et al. WO_3-based materials for photoelectrocatalytic glycerol upgrading into glyceraldehyde: Unravelling the synergistic photo- and electro-catalytic effects. *Appl. Catal. B Environ. Energy* **2022**, *318*, 121843.
42. Wang S, Liu G, Wang L. Crystal facet engineering of photoelectrodes for photoelectrochemical water splitting. *Chem. Rev.* **2019**, *119*, 5192–5247.
43. Zhang J, Zhang P, Wang T, Gong J. Monoclinic WO_3 nanomultilayers with preferentially exposed (002) facets for photoelectrochemical water splitting. *Nano Energy* **2015**, *11*, 189–195.
44. Ai J, Qin M, Xue M, Cao C, Zhang J, Kuklin AV, et al. Recent advances of photodetection technology based on main group III–V semiconductors. *Adv. Funct. Mater.* **2024**, *34*, 2408858.
45. Arumugam M, Yang H-H. A review of the application of wide-bandgap semiconductor photocatalysts for CO_2 reduction. *J. CO_2 Util.* **2024**, *83*, 102808.
46. Bellardita M, Loddo V, Augugliaro V, Palmisano L, Yurdakal S. Selective photocatalytic and photoelectrocatalytic synthesis of valuable compounds in aqueous medium. *Catal. Today* **2024**, *432*, 114587.
47. Song H, Luo S, Huang H, Deng B, Ye J. Solar-driven hydrogen production: Recent advances, challenges, and future perspectives. *ACS Energy Lett.* **2022**, *7*, 1043–1065.
48. Sun L, Han L, Huang J, Luo X, Li X. Single-atom catalysts for photocatalytic hydrogen evolution: A review. *Int. J. Hydrogen Energy* **2022**, *47*, 17583–17599.
49. Tang D, Lu G, Shen Z, Hu Y, Yao L, Li B, et al. A review on photo-, electro- and photoelectro-catalytic strategies for selective oxidation of alcohols. *J. Energy Chem.* **2023**, *77*, 80–118.